The Cerebellum
https://doi.org/10.1007/s12311-018-0945-2

ORIGINAL PAPER

Cerebellar-Stimulation Evoked Prefrontal Electrical Synchrony Is Modulated by GABA

Xiaoming Du[1] · Laura M. Rowland[1] · Ann Summerfelt[1] · Fow-Sen Choa[2] · George F. Wittenberg[3,4] · Krista Wisner[1] · Andrea Wijtenburg[1] · Joshua Chiappelli[1] · Peter Kochunov[1] · L. Elliot Hong[1]

Abstract

Cerebellar-prefrontal connectivity has been recognized as important for behaviors ranging from motor coordination to cognition. Many of these behaviors are known to involve excitatory or inhibitory modulations from the prefrontal cortex. We used cerebellar transcranial magnetic stimulation (TMS) with simultaneous electroencephalography (EEG) to probe cerebellar-evoked electrical activity in prefrontal cortical areas and used magnetic resonance spectroscopy (MRS) measures of prefrontal GABA and glutamate levels to determine if they are correlated with those potentials. Cerebellar-evoked bilateral prefrontal synchrony in the theta to gamma frequency range showed patterns that reflect strong GABAergic inhibitory function ($r = -0.66$, $p = 0.002$). Stimulation of prefrontal areas evoked bilateral prefrontal synchrony in the theta to low beta frequency range that reflected, conversely, glutamatergic excitatory function ($r = 0.66$, $p = 0.002$) and GABAergic inhibitory function ($r = -0.65$, $p = 0.002$). Cerebellar-evoked prefrontal synchronization had opposite associations with cognition and motor coordination: it was positively associated with working memory performance ($r = 0.57$, $p = 0.008$) but negatively associated with coordinated motor function as measured by rapid finger tapping ($r = -0.59$, $p = 0.006$). The results suggest a relationship between regional GABA levels and interregional effects on synchrony. Stronger cerebellar-evoked prefrontal synchrony was associated with better working memory but surprisingly worse motor coordination, which suggests competing effects for motor activity and cognition. The data supports the use of a TMS-EEG-MRS approach to study the neurochemical basis of large-scale oscillations modulated by the cerebellar-prefrontal connectivity.

Keywords TMS · Cerebellum · Cerebellar-frontal · MRS · Oscillation · EEG

Introduction

While a primary function of the cerebellum is feedback control of motor function, cerebellar-prefrontal circuitry also has been recognized as important in cognitive function [1, 2]. The cerebellum is well interconnected with prefrontal cortices in both feedforward and feedback directions [3–6]. Multiple, segregated fronto-cerebellar circuits have been characterized in nonhuman primates using transneuronal tracing techniques [7, 8] and in humans using functional connectivity magnetic resonance imaging (MRI) [9]. Transcranial magnetic stimulation (TMS) targeting the cerebellar cortex represents a novel way to modulate the excitability of remote cortical regions. TMS to the cerebellum has been shown to modulate the default mode network [10], attention networks [2, 10], and cerebellar functional connectivity with frontal and other regions [11]. Therefore, TMS provides a prospective approach to test the function of cerebellar-prefrontal circuitry. Unlike previous TMS cerebellar studies that focused on fMRI-based

Electronic supplementary material The online version of this article (https://doi.org/10.1007/s12311-018-0945-2) contains supplementary material, which is available to authorized users.

✉ Xiaoming Du
xdu@som.umaryland.edu

[1] Maryland Psychiatric Research Center, Department of Psychiatry, University of Maryland School of Medicine, P.O. Box 21247, Baltimore, MD 21228, USA

[2] Department of Electrical Engineering and Computer Science, University of Maryland Baltimore County, Baltimore, MD 21250, USA

[3] Department of Neurology, Physical Therapy and Rehabilitation Science, Internal Medicine, Older Americans Independence Center, University of Maryland, Baltimore, MD 21201, USA

[4] Department of Veterans Affairs (VA) Maryland Health Care System, Geriatrics Research, Education and Clinical Center, and Maryland Exercise & Robotics Center of Excellence, Baltimore, MD 21201, USA

Published online: 15 May 2018

assessments of regional brain networks, the purpose of this study was to measure modulation of the prefrontal circuitry oscillations using electroencephalography (EEG) when the cerebellum was stimulated. The electrophysiology-based prefrontal synchrony assessment provides a temporally precise assessment for the network response to cerebellar TMS.

Besides coordinating motor function through cerebellothalamocortical pathways [12, 13], the cerebellum likely supports higher cognitive functions. This is supported by transneuronal tracing methods in nonhuman primate showing the cerebellum projects to the dorsolateral prefrontal cortex (area 46), a region known for its role in higher order cognition [14–17]. Resting-state functional connectivity studies showed that the cerebellum can be divided into two subregions where the supramodal region is functionally correlated with prefrontal and posterior-parietal cortex [18, 19]. The cerebellum has been implicated in verbal working memory, language, executive, and emotional processing functions [16, 20–24]. For example, damage to the cerebellum impairs working memory [25]; transcranial direct current stimulation or TMS over the cerebellum has been shown to modulate verbal working memory [26–28]; and meta-analysis suggests lobule VI and Crus I of the cerebellum are involved in verbal working memory [17].

Theoretical modeling and nonhuman studies suggest that local and long-distance neural synchronization is regulated by the interactions between GABAergic and glutamatergic signaling [29, 30]. The contrasting GABAergic vs. glutamatergic control of synchronized oscillations is thought to be present in humans, but direct evidence remains elusive. Synchronized neuronal firing is part of the brain's mechanisms for coordination and integration of cognitive operations [31, 32]. Our approach is to use TMS over the cerebellum while recording synchronized electrical activity in prefrontal areas, and assess whether the synchronized electrical activities follow a pattern consistent with GABAergic inhibitory and glutamate-excitatory control of the prefrontal cortical synchrony.

We hypothesized that the relative balance of prefrontal glutamate and GABA levels would be associated with prefrontal electrical synchrony induced by stimulation to the cerebellar-prefrontal circuitry. To test this, TMS pulses with different levels of intensity were applied to posterior cerebellum and we used prefrontal EEG to assess cerebellar perturbed prefronto-prefrontal synchrony, and whether prefrontal glutamate/GABA modulated this synchrony. The combination of TMS and simultaneous EEG may allow a more direct assessment of cortical excitability and its oscillatory response compared to TMS and simultaneous fMRI [33–35]. GABA and glutamate levels were noninvasively measured by proton magnetic resonance spectroscopy (MRS) [36, 37]. Their levels are relatively stable within subjects but vary across individuals [38], which, combined with TMS/EEG, provide a means to estimate how variations in background tissue levels of glutamate/GABA chemistry modulate the prefrontal chemistry-electricity interaction.

Materials and Methods

Participants

Twenty medically and psychiatrically healthy volunteers (7 females, age 20–62 years) participated in the study. All subjects were interviewed with the Structured Clinical Interview for DSM-IV (SCID) to exclude psychiatric and substance abuse diagnosis. Potential subjects with major medical and neurological illnesses were also excluded. TMS screening interviews confirmed that none of the subjects had contraindications for TMS. All subjects gave written informed consent approved by the University of Maryland Baltimore Institutional Review Board.

Working Memory and Motor Coordination Tasks

All participants completed a working memory and a motor coordination task. Working memory capacity was assessed using the digit sequencing task [39]. Participants were presented with randomly ordered series of numbers that steadily increased length. They were asked to report the numbers in order, from lowest to highest. The number of trials in the correct order was recorded. Working memory was chosen as a behavioral indicator for prefrontal cognitive functioning. Strong GABAergic mediated prefrontal synchronization is thought to be critical for working memory [40, 41].

Motor coordination was indexed by using a finger tapping task, one of the most common paradigms to study human motor coordination [42, 43]. Subjects were instructed to use their dominant right-hand index finger to tap on a button as many times as possible in the 10-s period. This was repeated 10 times, with inter-trial intervals ≥ 1 min. Mean tapping scores were calculated as the number of taps per trial averaging across the ten trials. As good motor performance in this task requires highly automated motor control, it was expected that stronger prefrontal synchrony could actually interfere with this finger tapping task.

Magnetic Resonance Spectroscopy

Each participant completed a MRS scan prior to TMS assessment, including a structural MRI for TMS location navigation. Imaging data were collected using a Siemens 3T Trio scanner and a 32-channel head coil located at the University of Maryland Center for Brain Imaging Research. A T1-weighted structural MRI was obtained by a magnetization prepared sequence with an adiabatic inversion contrast-forming pulse (TE/TR/TI = 3.04/2100/785 ms, flip angle = 11 degrees) at isotropic spatial resolution of 0.8 mm. A retrospective motion-correction technique was used to reduce subject motion-related artifacts.

MRS was performed in three prefrontal cortex sites within the same scanning session: left, medial and right prefrontal areas (PFC) under electrodes F3, FZ and F4, respectively. The same size of voxel was used (all 4 × 3 × 2 cm or 24 ml) in all three sites but with orientation adjusted in left and right PFC to include as much cortical area as possible. Because the glutamate/GABA measurements from the three sites were found to be very similar in the initial subjects (see Results), only the medial prefrontal cortex (Fig. 1a) was sampled for the rest of the subjects to represent glutamate/GABA in the prefrontal cortex. The medial prefrontal area extensively connects to bilateral prefrontal areas [44, 45]. All MRS scanning and processing procedures were otherwise the same and the remaining descriptions focus only on the medial prefrontal cortex. For detection of glutamate, spectra were acquired using phase rotation STEAM: TR/TM/TE = 2000/10/6.5 ms, VOI ~ 6 cm^3, NEX = 256, 2.5 kHz spectral width, 2048 complex points, and phases: $\varphi_1 = 135°$, $\varphi_2 = 22.5°$, $\varphi_{13} = 112.5°$, $\varphi_{ADC} = 0°$ [46]. A water reference (NEX = 16) was also acquired for phase and eddy current correction as well as quantification. A basis set of 19 metabolites was simulated using the GAVA software package [47] (Fig. 1b). The basis set was imported into LCModel (6.3-0I) and used for quantification [48]. Only metabolites with mean standard deviations less than 20% were included in statistical analyses. Spectra with LCModel reported linewidths greater than 0.1 Hz and signal-to-noise ratio less than 10 were excluded from further analyses. We have shown that the short-TE STEAM method produces excellent reproducibility for glutamate and glutamine [49]. For detection of GABA, spectra were acquired from the same voxel using macromolecule suppressed MEGA-PRESS: TR = 2000, TE = 68 ms, 20.36 ms length and 44 Hz bandwidth full width at half maximum editing pulses applied at 1.9 (ON) and 1.5 (OFF) ppm, and 256 averages (128 ON and 128 OFF); water unsuppressed 16 averages [50]. MEGA-PRESS for GABA has established excellent reproducibility [38, 51]. GABA spectra were frequency and phase corrected and quantified with GANNET 2.0 toolkit, a MATLAB program specifically developed for analysis of GABA MEGA-PRESS spectra. Metabolite levels are reported in institutional units and corrected for the proportion of the gray matter, white matter, and cerebrospinal fluid within each spectroscopic voxel using in-house MATLAB code [52, 53]. The primary measure was the glutamate/GABA ratio, which was taken to index a potential biological signature for the excitatory/inhibitory balance. Association analyses with glutamate and GABA levels separately were also performed to further ensure that any significant findings on the glutamate/GABA ratio were consistent with the glutamate-excitatory vs. GABA-inhibitory hypothesis.

Transcranial Magnetic Stimulation

Single pulse TMS was administered over the posterior cerebellum, stereotactically localized using the individual's high resolution structural MRI (Fig. 1a). At the beginning of each TMS session, TMS to the left motor cortex (M1) was used to determine resting motor threshold (RMT), which was then

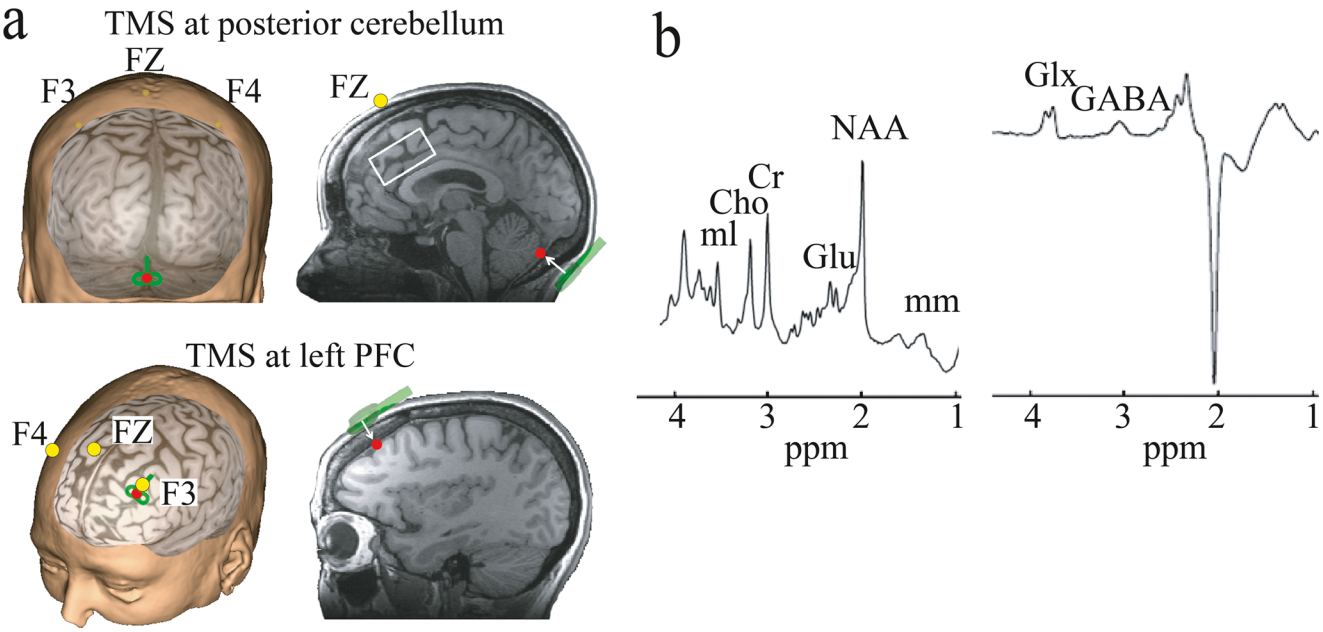

Fig. 1 TMS, MRS, EEG locations. **a** Illustrations of electrode positions (F3, F4, FZ) and the transcranial magnetic stimulation (TMS) sites at posterior cerebellum and left prefrontal cortex (green coils). Magnetic resonance spectroscopy (MRS) for GABA and glutamate (Glu) levels was obtained from a large medial frontal lobe voxel (white box) located below FZ. Yellow dot: EEG recording location. Red dot: TMS target. **b** An example of the MRS spectra for GABA and glutamate

Table 1 Associations of TMS-evoked prefrontal synchrony to neurochemicals and behavioral functions

Prefrontal PLV	Glutamate/ GABA ratio	Glutamate	GABA	Working memory	Motor coordination
Cerebellar stimulation					
Suprathreshold	+	n.s	−	+	−
Subthreshold	+	n.s	−		
Left PFC stimulation					
Suprathreshold	+	+	−		
Subthreshold	+	n.s	−		
Sham stimulation	n.s	n.s	n.s		
Resting state EEG	n.s	n.s	n.s		

TMS-evoked prefrontal phase locking value (PLV) was indexed by F3-F4 PLV. PFC: prefrontal cortex. EEG: electroencephalography. n.s indicates not significant. + indicates significant with positive correlations. − indicates significant with negative correlations

used to guide TMS stimulation intensity. For comparison, TMS was also applied to the left prefrontal cortex (PFC) (Fig. 1a). PFC stimulation provides an active control by locally affecting PFC-PFC synchrony, as compared to the cerebellum stimulation that aimed to affect the PFC-PFC synchrony remotely. All participants participated in both TMS sites and all TMS intensity levels including the shams.

Focal magnetic stimuli were given through a figure-eight coil (70 mm outer diameter of each wing) using Magstim 200 Magnetic stimulators with a 20-μs single pulse monophasic current waveform (Magstim Co., Whitland, UK). The anatomical images were imported into the Brainsight™ TMS Frameless Navigation system (Rogue Research Inc., Montreal, Canada) for precise coil positioning. For left motor cortex, the stimulus target for each participant was the scalp position above the left hemisphere (averaged MNI stereotaxic coordinates: −38, −11, 64) where TMS induced the maximum peak-to-peak motor evoked potential (MEP) amplitude from the right first dorsal interosseous muscle. The coil was held by a mechanical arm with the coil handle pointing backward and rotated 45° away from the midline to induce currents that traveled in a posterior-to-anterior direction across the central sulcus [54]. Participants were instructed to remain relaxed throughout the application of TMS, while the muscle was monitored for relaxation, confirmed by visual inspection of the EMG.

The TMS coil was pointed to the middle (i.e., along the midline) of the bilateral Crus I/II of the posterior cerebellum that has known connectivity to PFC BA 9 and 46 through thalamus [7, 13]. This location was defined as the midpoint of bilateral Crus I/II (averaged MNI stereotaxic coordinates: 0, −79, −26). Although other types of coils can be used to stimulate cerebellum, such as iron core coil [55, 56] or double cone coil [57–59], we selected the figure-of-eight coil for cerebellum stimulation as in many recent studies [e.g., 10, 11, 60–62]. The coil handle was pointing upward for posterior cerebellum stimulation. Participants were positioned in a chin-to-chest flexion position so that the posterior cerebellum was exposed as much as possible. This neck and coil relationship also reduced the chance of stimulating the occipital lobe and allowed positioning the coil to be as close to the posterior cerebellum as possible. Although the MRI images and a neuronavigation system were used to ensure the precise positioning of the coil, we also checked for accidental stimulation to the occipital lobe by asking participants after the experiment whether they perceived phosphenes, which is an indication of visual cortex TMS stimulation [63, 64]. Only two out of 20 participants reported possible perception of phosphenes, and both reported that the possible phosphenes occurred only rarely during the suprathreshold stimulations.

Left PFC was defined at the junction of the middle and anterior thirds of the middle frontal gyrus by neuronavigation using each participant's MRI (averaged MNI stereotaxic coordinates: −39, 33, 38), corresponding to the junction between posterior regions of Brodmann area (BA) 9 and the superior section of BA 46 [65, 66]. The coil was held with the coil handle pointing backward. The participant was sitting in an upright position with chin-rest and two head-supports were used to stabilize the head during PFC TMS.

Sham TMS was conducted by delivering the same suprathreshold stimulation while turning the TMS coil 90° and moving it away from skull (1~2 cm). The sounds of TMS stimulation were mostly preserved while delivering a highly attenuated magnetic pulse to the brain. Participants wore earplugs to muffle the sounds in all conditions, although the sounds remained audible in all conditions and as such, the sham condition resembled a non-TMS, auditory stimulation condition. Two subjects' sham condition data were not recorded due to technical problems.

For each site, suprathreshold (120% RMT), subthreshold (80% RMT) and sham TMS were delivered in separate blocks, with the order of the blocks randomized across subjects. The effects of TMS intensity can be evaluated by comparing suprathreshold and subthreshold conditions. There

were 60 TMS repetitions in one block for each TMS intensity and sham in each TMS location. The inter-trial intervals with each block ranged from 4 to 10 s. Blocks were separated by about 5 min.

Resting Motor Threshold (RMT) and Electromyography (EMG) Recording

Surface electromyography (EMG) was recorded from the right first dorsal interosseous (FDI) muscle with Ag/AgCl disc electrodes (CareFusion Inc., Middleton, WI) placed in a tendon-belly montage. A ground electrode was placed over the right ulnar styloid. EMG was recorded with a NeuroScan Synamp2 amplifier (Charlotte, NC) amplified (gain of 10) and sampled at 5 kHz [67–69]. Peak-to-peak amplitude of the motor-evoked potentials was measured. RMT was defined according to conventional criteria as the minimum intensity needed to elicit a MEP of >50 μV in at least 5 out of 10 consecutive stimuli. RMT is reported as a percentage of the maximum stimulator output. RMT was identified using left M1 stimulations. The averaged RMT was 46.5 ± 7.1% of maximum output of the Magstim 200 Magnetic stimulator.

Electrophysiology

TMS-evoked potential was recorded using a Neuroscan SynAmp2 (Charlotte, NC) and an electrode cap designed for accommodating the simultaneous TMS/ERP experiment. The electrodes F3, FZ, and F4 were used according to the extended 10–20-system of electrode positions (Fig. 1a). The locations of the electrodes were digitized with an optical tracking system (Brainsight, Rogue Research Inc., Montreal, Canada) and superimposed on a three-dimensional MRI scan of the subject's head. TMS-related EEG was recorded at a 1 kHz sampling rate with bandpass filtering at 0.1–200 Hz. The ground electrode was placed on the forehead. A nose electrode served as a reference. Electrode impedance was kept below 5 kΩ. Saturation of the EEG amplifiers by the TMS pulse was prevented by using the de-blocking function 4 ms before and 4 ms after each TMS pulse through a sample-and-hold circuit that pinned the amplifier output below the maximum level. Potential electrode polarizations were minimized by using non-polarizable Ag/AgCl electrodes [70]. The offline analysis was conducted by using Scan 4.3 software (Neurosoft, Inc., EI Paso, TX) and MATLAB (MathWorks, Inc., Natick, MA). Resting EEG was recorded in a 5-min session with eyes open at baseline without TMS and participants were asked to relax. Resting EEG was epoched every 4.3–4.6 s and was otherwise processed using the same data processing procedures. The resting EEG was employed to assess if there were associations between neural oscillations and neural chemicals during resting.

Eye-blink artifacts on the EEG were removed using a VEOG-based eye-blink spatial filter routine implemented in Neuroscan software [71]. In this EOG correction method, the proportion of signals removed from EEG channels are estimated from the eye movement averages which increase the accuracy of EOG correction. Records were then filtered at 1–100 Hz in 24db/octaves, epoched from −1000 to 2800 ms pre- and post-TMS, baseline-corrected, threshold-filtered at ±400 μV for any additional TMS artifact rejection, followed by visual inspection to exclude any missed artifacts from muscle contractions. Prefrontal phase-synchrony was defined by a metric of the difference between phase values of the single trial neural oscillations across two locations, in the 1–50 Hz range. To extract single-trial oscillatory responses, the artifact-free EEG records were filtered at 1–50 Hz. A long epoch was used to minimize edge effects. The continuous complex Morlet wavelet transform (CWT) was applied to each trial to decompose the oscillatory activities. We quantified the prefrontal interhemispheric phase locking between F3 and F4 electrodes by computing the phase-locking value (PLV) [32, 72] across the whole trial from 1 to 50 Hz. The PLV for two recording channels m and n at a particular center frequency f_0 and time t is defined as

$$PLV_{mn}(t,f_0)=\frac{1}{K}\left|\sum_{k=1}^{K}e^{i\left(\varphi_k^m(t,f_0)-\varphi_k^n(t,f_0)\right)}\right|$$

Where K denotes the number of trials, and $\varphi_k^m(t,f_0)$ and $\varphi_k^n(t,f_0)$ denote the instantaneous phases of the two channels that were computed during the k-th trial using the wavelet transform with center frequency f_0. Thus, the PLV ranged from 0 to 1. The higher the phase similarity between these two electrodes, the higher the PLV. PLV close to zero indicates lack of phase alignment of the two electrodes and PLV close to 1 indicates that phase value at one electrode closely matches the phase value of the other electrode.

Data Analyses

Comparisons of glutamate/GABA ratios among brain regions were made using repeated measures ANOVA. The synchrony between bilateral frontal areas was represented by the PLVs between F3 and F4 electrodes on single trials, which were then averaged across subjects to generate PLV time-frequency maps. The relationships between PLV time-frequency maps and glutamate/GABA ratio were then assessed using a Pearson's correlation matrix, which yielded maps representing the strength of the correlations across time and frequency. To identify cluster(s) that represent statistically significant PLV and glutamate/GABA correlations after controlling the family-wise error rate, we adopted a cluster-based permutation test approach [73]. In this approach, the correlation coefficients (r) and corresponding significance level (p) between PLV and glutamate/GABA levels

were computed for each time and frequency point, which yields a time-frequency map. For each map, a threshold was set ($p < 0.05$) to identify formation of segregated clusters within the map, where r values at adjacent time or frequency points were summed to produce a cluster-level r value for each cluster. To determine whether these cluster values were formed above chance at >99%, we used permutation with 1000 repetitions by randomly assigning glutamate/GABA ratio values to each participant and calculating the PLV and glutamate/GABA correlations. To use maximum cluster-level statistics [74, 75], the most extreme cluster-level r values from each of the 1000 permutations were used to derive a null hypothesis distribution. The p value of each cluster was derived from its ranking in this null hypothesis distribution and the significance level (α) was set at < 0.01. To further account for multiple correlation maps, the false discovery rate (FDR) method was applied to obtain corrected p value after correcting for the number of correlation maps. Finally, to visualize the PLV and glutamate/GABA relationship within the significant clusters, mean PLV values within the clusters were plotted against the glutamate/GABA ratio values using scatter plots. The same process was repeated for glutamate and GABA separately. Age was regressed out for behavior performances, and the residuals were used to test associations with glutamate/GABA and PLV measures.

Results

Left, Medial and Right Frontal Glutamate/GABA Levels

Repeated measures ANOVA was used to compare glutamate/GABA levels among three areas (left, medial, and right PFC) in six individuals. There was no significant effect of location ($F(2, 9.34) = 0.82$, $p = 0.47$), suggesting a similar basal glutamate/GABA composition across the PFC sites. As such, MRS for the remaining participants was obtained only from the mPFC site under FZ (Fig. 1).

Associations Between Frontal Glutamate/GABA and TMS-Evoked Oscillations by Cerebellar Stimulation

The relationship between glutamate/GABA and cerebellar-stimulation evoked oscillations was explored by calculating a Pearson correlation between glutamate/GABA ratio and the PLV map. We examined TMS-evoked oscillations and calculated PFC synchrony by computing PLV [32, 72] across 1 to 50 Hz between bilateral PFC electrodes (F3 and F4) (Fig. 2c and d) when the posterior cerebellum was stimulated. Prefrontal glutamate/GABA ratio was significantly associated with suprathreshold cerebellar-evoked PFC-PFC synchrony ($r = 0.67, p = 0.001$) in a wide frequency range (4–50 Hz), where the significant frequency and time areas were defined by the cluster-based permutation test (Fig. 2h and i). Within this statistically significant broadband, the stronger association was in the alpha and beta frequency range at 9–25 Hz ($r = 0.79, p = 0.0003$; this and all reported significant clusters below were significant after FDR correction for multiple comparisons).

Exploring glutamate and GABA levels separately, there was a negative correlation between GABA and cerebellar-evoked PFC synchrony in the 11–45 Hz range ($r = -0.66$, $p = 0.002$) (Fig. 2m and n) as defined by the cluster-based permutation tests, while glutamate showed no significant relationship ($r = 0.24$, n.s.) (Fig. 2r and s; Table 1). Therefore, the ratio effect mainly reflects a negative relationship with GABA, which is consistent with a GABAergic inhibitory effect on phase-locked synchrony.

Similar results were found with subthreshold stimulation (Fig. 2c, g, l, q; Table 1). Thus, GABA was strongly and inversely related to PFC alpha-beta-gamma synchrony when evoked by the cerebellar stimulation.

Further comparisons were made using PFC synchrony from resting state EEG (5 min EEG recording without TMS; Fig. 2a), which showed only weak PFC-PFC PLV that was not significantly correlated with glutamate/GABA, GABA, or glutamate (Fig. 2e, j, o; Table 1). No significant correlations were found during sham stimulation (Fig. 2f, k, p) (all corrected $p > 0.05$; Table 1). Thus, oscillations evoked by cerebellar TMS appear to reveal the relationship between PFC synchronization and glutamate/GABA ratio.

Associations Between Frontal Glutamate/GABA and TMS-Evoked Oscillations by Left PFC Stimulations

When left PFC was stimulated by suprathreshold TMS, the glutamate/GABA ratio was also significantly associated with PFC evoked PFC-PFC synchrony ($r = 0.62$, $p = 0.004$) in 4–48 Hz, where the frequency and time area was defined by the cluster-based permutation test (Fig. 3d and e). Within this statistically significant broadband, the stronger association was at the theta to low beta frequency range at 4–16 Hz ($r = 0.72$, $p = 0.0004$).

Taking glutamate and GABA levels separately, there was a negative correlation between GABA and PLV in the theta to beta frequency (clustered at 4–16 Hz; $r = -0.65$, $p = 0.002$) (Fig. 3g and h; Table 1) and a positive correlation between glutamate and PLV in 5–13 Hz range ($r = 0.66$, $p = 0.002$) (Fig. 3j and k; Table 1). Therefore, the ratio effect reflected both a positive relationship with glutamate and a negative relationship with GABA, and as such the relationships are consistent with the opposing GABAergic-inhibitory vs. glutamatergic-excitatory hypothesis, involving a broad band that was most robust at the theta to beta range. Similar, but weaker correlations were found during subthreshold TMS (Fig. 3c, f, i; Table 1).

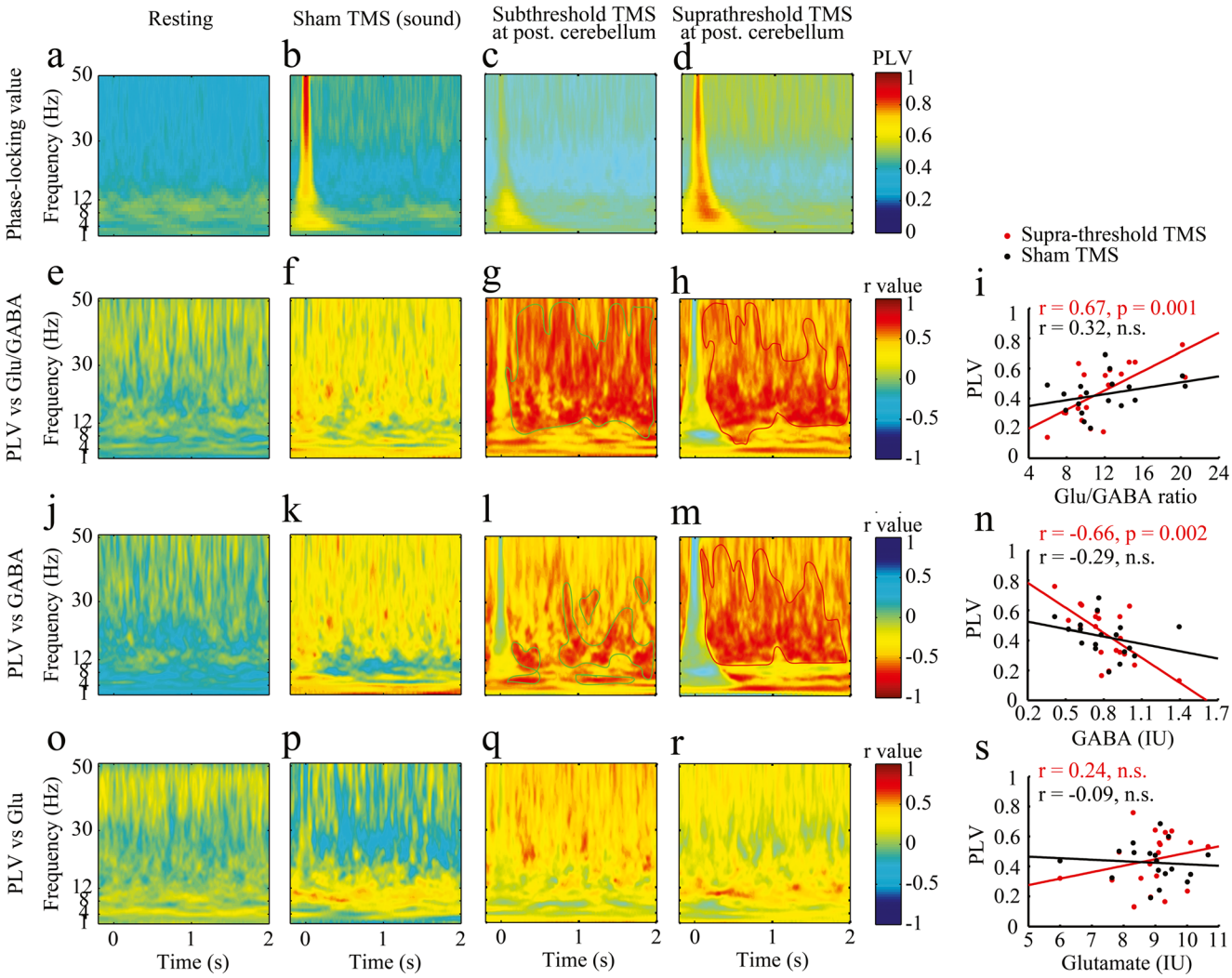

Fig. 2 Cerebellar TMS evoked prefrontal phase sychroniztion and neurochemistry. Prefrontal phase-locking values (PLV) in resting (recorded before TMS) (**a**), sham (sound only) (**b**), subthreshold cerebellar TMS (**c**), and suprathreshold cerebellar TMS (**d**). x-axis: time; y-axis: frequency. First row: Heat maps are time-frequency maps of the F3-F4 PLV values (**a**–**d**). Second row: Heat maps of correlations between glutamate/GABA ratio and the four conditions: resting (**e**), sham (**f**), subthreshold TMS (**g**), and suprathreshold TMS (**h**). Statistically significant correlations after correction for multiple comparisons were found in a 4–48 Hz cluster (red enclosure) under suprathreshold TMS with GABA. The mean values from the significant cluster are plotted to aid visual inspection (**i**). For comparison purposes, the mean PLV values from the sham conditoin were also plotted using the same cluster boundary (black data points). A similar pattern with smaller clusters was observed under subthreshold TMS (green enclosure) with Glu/GABA ratio (**g**) and GABA (**l**), but not with glutamate (**q**). Third row: Correlations between GABA level and PLV (**j**–**n**). Fourth row: Correlations between glutamate and PLV (**o**–**s**). Note that the color scales for GABA and glutamate are reversed to facilitate direct comparisons of correlation strength

Different Relationships of Cerebellar TMS Evoked Prefrontal Synchrony to Working Memory and Motor Coordination

The functional role of prefrontal synchrony was explored by estimating the association between prefrontal synchrony and behavioral assessments (i.e., working memory and motor coordination performance). Glutamate/GABA ratio or GABA and glutamate levels themselves were not correlated with working memory or finger tapping scores (all $p > 0.05$); but cerebellum TMS-evoked PFC synchrony was positively associated with working memory in theta, low beta and gamma frequency bands ($r = 0.57$, $p = 0.008$) (Fig. 4a and b; Table 1), suggesting that PLV may have a more direct relationship with working memory than glutamate/GABA. In comparison, cerebellum TMS-evoked PFC synchrony was negatively correlated with finger tapping scores in alpha, beta and low gamma frequency bands ($r = -0.59$, $p = 0.006$) (Fig. 4c and d; Table 1), supporting that cerebellum TMS-evoked PFC synchrony may have opposite effects on working memory vs. motor coordination. No such correlations were found with PFC TMS-evoked synchrony (all $p > 0.05$).

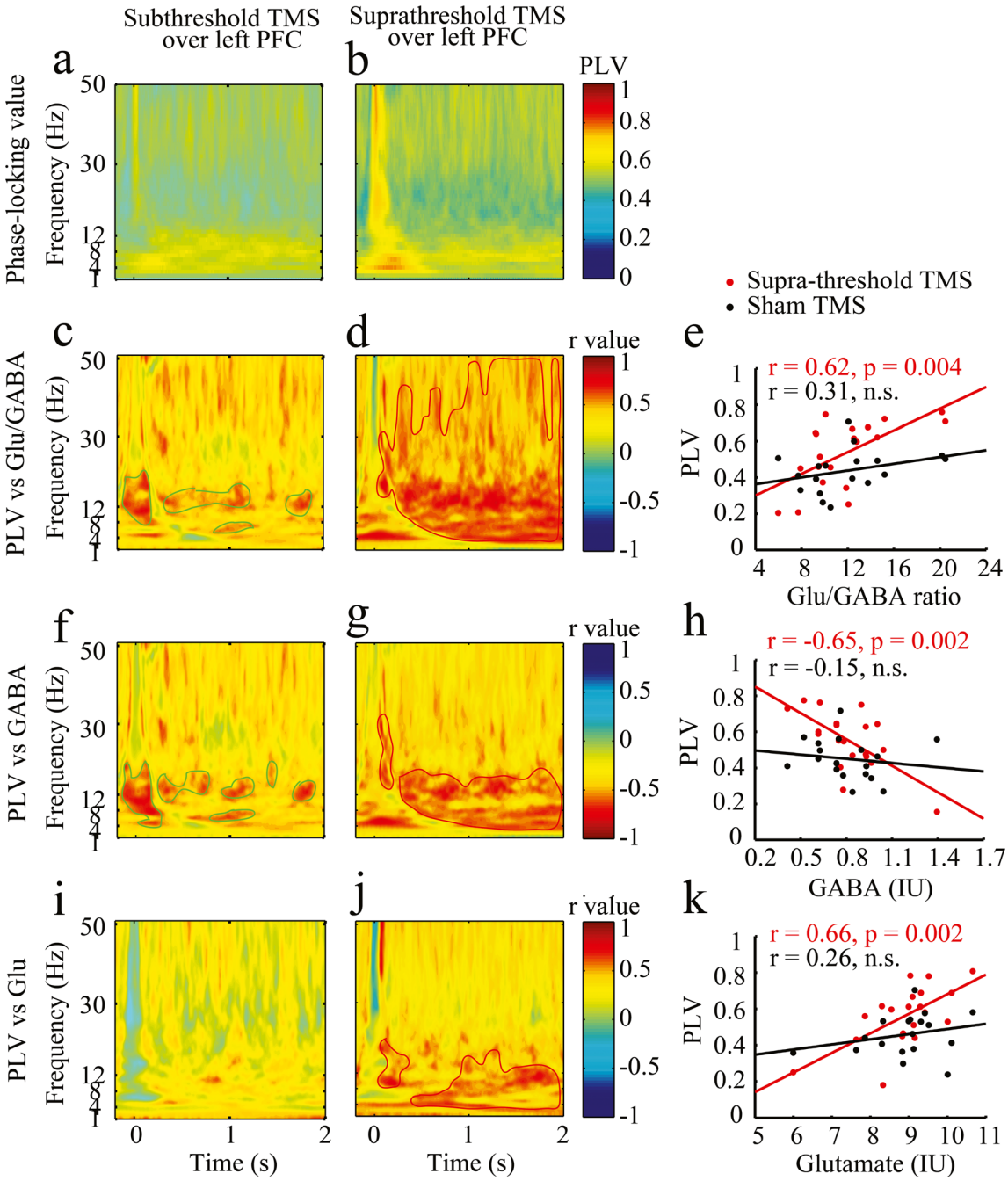

Fig. 3 Left prefrontal cortex TMS evoked prefrontal phase sychronization and neurochemistry. Prefrontal phase-locking values (PLV) in subthreshold TMS (**a**), and suprathreshold TMS (**b**). x-axis: time; y-axis: frequency. First row: Heat maps are time-frequency maps of the F3-F4 PLV values (**a** and **b**). Second row: Heat maps of correlations between glutamate/GABA ratio and the subthreshold TMS (**c**) and suprathreshold TMS (**d**). Statistically significant correlations after correction for multiple comparisons were found in a 4–50 Hz cluster (red enclosure) under suprathreshold TMS with glutamate/GABA ratio (**d**). The mean values from the significant cluster are plotted to aid visual inspection (**e**). For comparison purposes, the mean PLV values from the sham conditoin were also plotted using the same cluster boundary (black data points). Similar pattern with smaller clusters was observed under subthreshold TMS (green enclosure) with glutamate/GABA ratio (**c**). Third row: Correlations between GABA level and PLV (**f**–**h**). Fourth row: Correlations between glutamate and PLV (**i**–**k**). Note that the color scales for GABA and glutamate are reversed to facilitate direct comparisons of correlation strength

Discussion

The cerebellum is known to project via the thalamus to multiple cortical areas, such as motor, prefrontal, and posterior-parietal cortices [7, 8, 13, 76, 77]. Cerebellar TMS stimulation send signals to the PFC through cerebellar-thalamic-prefrontal cortical circuit and reflected by the observed PFC-PFC synchrony. Interestingly, the PFC synchrony induced by this

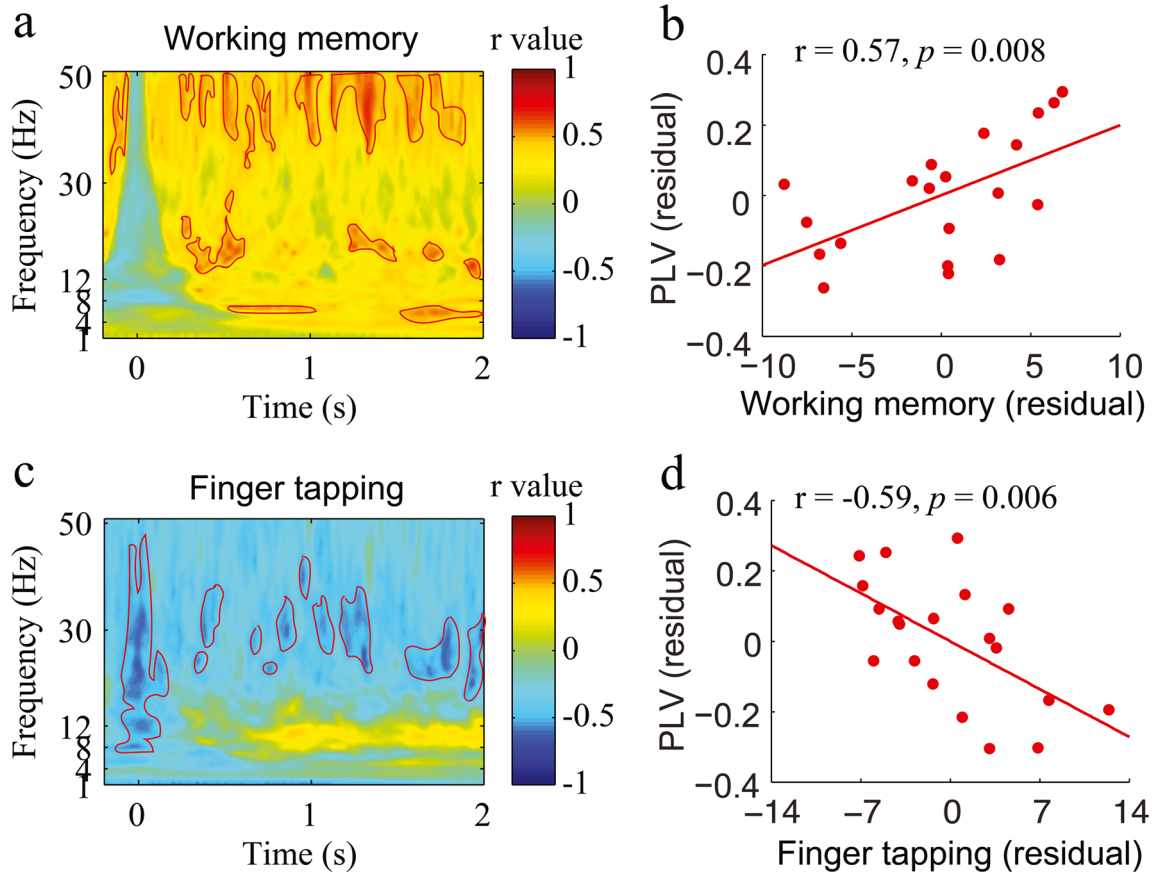

Fig. 4 Working memory and finger tapping associations with cerebellar TMS evoked phase locking value (PLV). Pearson's correlations between PLV time-frequency and working memory were shown in the time-frequency maps. Time-frequency components that were statistically significant are in a dark red color, mostly in theta, low beta and gamma band ranges (**a**). Most of the significant correlations between PLV and finger tapping fell within alpha, beta and low gamma frequency bands (**c**). To show the direction of the correlations, the PLV values from all of the significant PLV-working memory time-frequency components in panel (**a**) were extracted and plotted against working memory performance. All measures were residuals after age was covariated out: individuals with higher working memory functions were associated with stronger TMS-evoked prefronto-prefrontal synchronization (**b**). Individuals with higher finger tapping performance were associated with weaker TMS-evoked prefronto-prefrontal synchronization (**d**)

stimulation was strongly predicted by basal PFC glutamate/GABA ratio ($r = 0.67$). Since TMS was delivered to the cerebellum, this chemical-electrical association likely reflects a long-range circuitry-based effect rather than a local TMS induced secondary effect [78].

Repeating the experiment using local PFC TMS, a similarly strong PFC glutamate/GABA ratio vs. PFC synchrony relationship was observed ($r = 0.62$). Regardless of the location of TMS, the induced PFC synchrony was negatively correlated with GABA levels ($r = -0.66$ and -0.65 for cerebellum and PFC TMS induced synchrony, respectively), where higher basal PFC GABA levels were associated with lower PFC synchrony. The results are consistent with the hypothesis that a PFC GABAergic inhibitory effect in humans can be indexed by TMS evoked PFC synchrony regardless of whether the input source is remote (cerebellum) or local (PFC).

Two levels of TMS intensity were utilized to evaluate the TMS strength required for effective stimulation of the PFC and cerebellum. In the present study, a similar pattern of results occurred with subthreshold (80% RMT) and suprathreshold (120% RMT) stimulations (Fig. 2g, h, l, m, q and r; Fig. 3c, d, f, g, i and j). As suprathrehsold stimulations usually induce larger discomfort than subthreshold stimulation, the similar pattern of results indicates that these findings are unlikely due to TMS induced discomforts. Moreover, the effective subthreshold stimulation has been demonstrated in the previous research [79]. Research also strongly supports that a subthreshold pulse may facilitate (intracortical facilitation) or inhibit (intracortical inhibition) following a suprathreshold pulse with the proper inter-stimulus intervals [67, 80, 81]. These results suggest that even subthreshold stimulation could effectively stimulate cerebellum.

Synchronized network oscillations are among the most preserved phenotypes in brain evolution [82]. Neural synchrony can self-organize to preserve input traces even after the input has ceased in support of cognitive operations [82, 83]. TMS-induced effects are known to have large inter-individual differences [84–86]. Here we show that a proportion of TMS-

induced synchronized response variance can be explained by the glutamate/GABA ratio with stimulation input specificity: while GABA levels were negatively correlated with the synchronized PFC response regardless of inputs from cerebellum vs. PFC, glutamate levels were positively correlated with synchronized response primarily from local PFC TMS.

Reciprocal cortico-cortical glutamatergic projections, regulated by inhibitory neurons are thought to mediate cross-regional synchrony [87, 88]. High levels of GABA may favor local effects and allow each region to inhibit incoming activity [68, 87, 88], resulting in reduced synchronized output. Although it's not fully clear how local GABA concentrations affect TMS evoked synchrony, one possible explanation is that high local GABA levels inhibits the spread of TMS evoked activities, further leading to a lower synchronization. The relationship with glutamate seems to be in the opposite direction. The observed relationships between glutamate/GABA ratio and synchrony are also consistent with the idea that cortical excitation is glutamatergic while lateral inhibition of the excitation is mediated by local inhibitory GABAergic inputs that control the spread of synchronized oscillations in the cortex [89, 90].

TMS stimulation may improve synchronized activity from the stimulated area to other regions [91]. Halko et al. (2014) showed that intermittent TBS over the lateral cerebellum substantially changed the functional connectivity between the cerebellum and medial prefrontal cortex [10]. Schutter and colleagues stimulated the medial cerebellum with repetitive TMS and found a shift in the anterior asymmetry of the gamma frequency band at the prefrontal cortex [92]. Single-pulse cerebellar TMS has also been shown to modulate frontal EEG activity [56]. Furthermore, the role of the cerebellum in cognitive performance has been well demonstrated [e.g., 2, 23], especially in working memory [93–99]. For example, single-pulse TMS over cerebellum in healthy individuals during the encoding phase of a verbal working memory task resulted in increased reaction times for the working memory [28]. Transcranial direct current stimulation (tDCS) over the cerebellum also impaired the practice-dependent improvement in verbal working memory [26]. Consistent with the literature, we found that cerebellar TMS evoked PFC PLVs at theta, low beta, and gamma bands were associated with better working memory performance. This suggests that cerebellar modulation of PFC synchronization may contribute to working memory performance (Fig. 4a and b).

Interestingly, cerebellar TMS-evoked PFC PLV at alpha to gamma bands was *negatively* associated with finger tapping scores. This task involves engagement of brain areas that include the primary sensorimotor cortices, supplementary motor area, premotor cortex, inferior parietal cortices, basal ganglia, and cerebellum, thought to responsible for rapid, automated motor coordination [42, 100]. Individuals with stronger cerebellum-evoked PFC synchronization at high beta band tended to have poorer self-paced finger tapping task performance (Fig. 4c and d). One interpretation is that high capacity for cerebellar-evoked PFC synchronization is required to perform working memory, but may interfere with a primarily motor task that requires automated performance. The negative correlation between cerebellar-evoked PFC synchronization and finger tapping performance is also consistent with the known phenomenon of cerebellum-brain inhibition [101]. For instance, Ugawa et al. showed that TMS over the contralateral cerebellar hemisphere decreases the excitability of primary motor cortex for 5–7 ms after the stimulation [102]. The opposite roles of cerebellar TMS-evoked PFC synchronization highlight the different circuit-level requirements for performance of working memory that requires maintaining information over time vs. a simple motor task with a speed requirement.

Some limitations of this study include a potential confound in that TMS may change local chemical levels [103–105]. Such changes have been previously found to be small (in 0 to 10% range) [103, 104] and should not primarily contribute to the strong glutamate/GABA and PLV correlations. PFC chemistry-synchrony patterns revealed by cerebellar TMS were even less likely caused by TMS induced PFC GABA changes. GABA and glutamate were measured in mPFC under FZ, but not under other PFC regions. We took this approach because this mPFC area has extensive fibers to bilateral PFC in primates [44], and initial data showed that there were no significant differences in glutamate/GABA levels in left, right, and medial PFC. Future studies measuring MRS from additional PFC areas could clarify the distribution of GABA and glutamate at different parts of the prefrontal cortex. We should also note that GABA and glutamate are not the only neurotransmitters regulating synchronized networks. For example, cholinergic neurotransmitters have been shown to influence neural oscillations [106, 107]. Furthermore, MRS cannot differentiate between intracellular vs. extracellular pools of GABA and glutamate, but instead measures total tissue levels. Additional work is needed to understand the relationship between overall levels and the presumed GABAergic vs. glutamatergic signaling. Another limitation was that we did not use the occipital lobe as a control. Although few participants reported possible phosphenes during the suprathreshold stimulations, it is still possible that rTMS may have stimulated the occipital cortex, which may lead to a cortico-cortical interaction between occipital and frontal areas [108]. However, previous studies comparing rTMS to medial cerebellum vs. occipital lobe showed that rTMS to cerebellum, but not occipital lobe, altered prefrontal gamma band [92]. The potential artifacts induced by volume conduction or cranial muscle contraction could also be confounds, although such sources cannot fully explain the results. Those artifacts were mainly within 200 ms after delivering TMS pulse (e.g., Figs. 2d and 3b), but most of the significant

clusters were after 200 ms (e.g., Fig. 2g, h, l and m). Finally, the observed associations between MRS indices and neural synchrony could be driven by a third unknown variable. This is possible especially for cerebellum stimulation, because the modulation from cerebellum to frontal cortex needs to pass through subcortical regions (e.g., thalamus) and those subcortical regions could affect the observed relationship. Future studies stimulating subcortical areas with deep brain stimulation techniques may help to clarify the current results.

We tested how cerebellar inputs may impact the prefrontal synchrony and its modulation by basal glutamate/GABA levels using a relatively new TMS-EEG-MRS approach. We further demonstrated that the cerebellar-evoked prefrontal synchrony is likely functionally relevant in influencing brain functions from higher order cognition to basic motor coordination. The opposing GABAergic-inhibitory vs. glutamatergic-excitatory relationship has been extensively described in basic neuroscience literature although its direct demonstration in human studies remains rare [109, 110]. The robust inverse association between GABA and prefrontal interhemispheric synchrony supports the basic principle of GABAergic inhibition affecting the spread of oscillations in human brains [111–113]. Using TMS-induced EEG to assess chemical-electrical interactions may lead to a better understanding of the mechanisms underlying neural synchrony in humans.

Acknowledgements LEH has received or plans to receive research funding or consulting fee on research projects from Mitsubishi, Your Energy Systems LLC, Neuralstem, Taisho, Heptares, Pfizer, Sound Pharma, Takeda, and Regeneron. All other authors declare no conflict of interest.

Funding Support was received from NIH grants MH085646, MH103222, MH108148, MH067533, a NARSAD award, State of Maryland contract (M00B6400091), and a generous private philanthropic donation from the Clare E. Forbes Trust.

References

1. Engelhardt E. Cerebrocerebellar system and Turck's bundle. J Hist Neurosci. 2013;22(4):353–65.
2. Esterman M, Thai M, Okabe H, DeGutis J, Saad E, Laganiere SE, et al. Network-targeted cerebellar transcranial magnetic stimulation improves attentional control. NeuroImage. 2017;156:190–8.
3. Schmahmann JD, Pandya DN. The cerebrocerebellar system. Int Rev Neurobiol. 1997;41:31–60.
4. Ernst TM, Thurling M, Muller S, Kahl F, Maderwald S, Schlamann M, et al. Modulation of 7 T fMRI signal in the cerebellar cortex and nuclei during acquisition, extinction, and reacquisition of conditioned Eyeblink responses. Hum Brain Mapp. 2017;38(8):3957–74.
5. Kansal K, Yang Z, Fishman AM, Sair HI, Ying SH, Jedynak BM, et al. Structural cerebellar correlates of cognitive and motor dysfunctions in cerebellar degeneration. Brain. 2017;140(3):707–20.
6. King M, Hernandez-Castillo C, Diedrichsen J. Towards a multi-function mapping of the cerebellar cortex. Brain. 2017;140(3):522–4.
7. Middleton FA, Strick PL. Anatomical evidence for cerebellar and basal ganglia involvement in higher cognitive function. Science (New York, NY). 1994;266(5184):458–61.
8. Middleton FA, Strick PL. Cerebellar projections to the prefrontal cortex of the primate. J Neurosci. 2001;21(2):700–12.
9. Krienen FM, Buckner RL. Segregated fronto-cerebellar circuits revealed by intrinsic functional connectivity. Cereb Cortex. 2009;19(10):2485–97.
10. Halko MA, Farzan F, Eldaief MC, Schmahmann JD, Pascual-Leone A. Intermittent theta-burst stimulation of the lateral cerebellum increases functional connectivity of the default network. J Neurosci Off J Soc Neurosci. 2014;34(36):12049–56.
11. Rastogi A, Cash R, Dunlop K, Vesia M, Kucyi A, Ghahremani A, et al. Modulation of cognitive cerebello-cerebral functional connectivity by lateral cerebellar continuous theta burst stimulation. NeuroImage. 2017;158:48–57.
12. Ito M. The cerebellum and neural control. New York: Raven Press; 1984.
13. Kelly RM, Strick PL. Cerebellar loops with motor cortex and prefrontal cortex of a nonhuman primate. J Neurosci Off J Soc Neurosci. 2003;23(23):8432–44.
14. Gordon N. The cerebellum and cognition. Eur J Paediatr Neurol. 2007;11(4):232–4.
15. Buckner RL. The cerebellum and cognitive function: 25 years of insight from anatomy and neuroimaging. Neuron. 2013;80(3):807–15.
16. Van Overwalle F, Baetens K, Marien P, Vandekerckhove M. Social cognition and the cerebellum: a meta-analysis of over 350 fMRI studies. NeuroImage. 2014;86:554–72.
17. Stoodley CJ, Schmahmann JD. Functional topography in the human cerebellum: a meta-analysis of neuroimaging studies. NeuroImage. 2009;44(2):489–501.
18. Balsters JH, Laird AR, Fox PT, Eickhoff SB. Bridging the gap between functional and anatomical features of cortico-cerebellar circuits using meta-analytic connectivity modeling. Hum Brain Mapp. 2014;35(7):3152–69.
19. O'Reilly JX, Beckmann CF, Tomassini V, Ramnani N, Johansen-Berg H. Distinct and overlapping functional zones in the cerebellum defined by resting state functional connectivity. Cereb Cortex. 2010;20(4):953–65.
20. Stoodley CJ, Schmahmann JD. The cerebellum and language: evidence from patients with cerebellar degeneration. Brain Lang. 2009;110(3):149–53.
21. Pleger B, Timmann D. The role of the human cerebellum in linguistic prediction, word generation and verbal working memory: evidence from brain imaging, non-invasive cerebellar stimulation and lesion studies. Neuropsychologia. 2018 (in press).
22. LaBar KS, Gitelman DR, Parrish TB, Mesulam MM. Neuroanatomic overlap of working memory and spatial attention networks: a functional MRI comparison within subjects. NeuroImage. 1999;10(6):695–704.
23. Chen SH, Desmond JE. Cerebrocerebellar networks during articulatory rehearsal and verbal working memory tasks. NeuroImage. 2005;24(2):332–8.
24. Tomasi D, Chang L, Caparelli EC, Ernst T. Different activation patterns for working memory load and visual attention load. Brain Res. 2007;1132(1):158–65.
25. Ravizza SM, McCormick CA, Schlerf JE, Justus T, Ivry RB, Fiez JA. Cerebellar damage produces selective deficits in verbal working memory. Brain. 2006;129:306–20.
26. Ferrucci R, Marceglia S, Vergari M, Cogiamanian F, Mrakic-Sposta S, Mameli F, et al. Cerebellar transcranial direct current stimulation impairs the practice-dependent proficiency increase in working memory. J Cogn Neurosci. 2008;20(9):1687–97.

27. Boehringer A, Macher K, Dukart J, Villringer A, Pleger B. Cerebellar transcranial direct current stimulation modulates verbal working memory. Brain Stimul. 2013;6(4):649–53.
28. Desmond JE, Chen SH, Shieh PB. Cerebellar transcranial magnetic stimulation impairs verbal working memory. Ann Neurol. 2005;58(4):553–60.
29. Stelzer A, Wong RK. GABAA responses in hippocampal neurons are potentiated by glutamate. Nature. 1989;337(6203):170–3.
30. Whittington MA, Traub RD, Jefferys JG. Synchronized oscillations in interneuron networks driven by metabotropic glutamate receptor activation. Nature. 1995;373(6515):612–5.
31. Engel AK, Fries P, Singer W. Dynamic predictions: oscillations and synchrony in top-down processing. Nat Rev Neurosci. 2001;2(10):704–16.
32. Liebe S, Hoerzer GM, Logothetis NK, Rainer G. Theta coupling between V4 and prefrontal cortex predicts visual short-term memory performance. Nat Neurosci. 2012;15(3):456–62. S1-2
33. Rosanova M, Casali A, Bellina V, Resta F, Mariotti M, Massimini M. Natural frequencies of human corticothalamic circuits. J Neurosci. 2009;29(24):7679–85.
34. Thut G, Veniero D, Romei V, Miniussi C, Schyns P, Gross J. Rhythmic TMS causes local entrainment of natural oscillatory signatures. Curr Biol. 2011;21(14):1176–85.
35. Kawasaki M, Uno Y, Mori J, Kobata K, Kitajo K. Transcranial magnetic stimulation-induced global propagation of transient phase resetting associated with directional information flow. Front Hum Neurosci. 2014;8:173.
36. Puts NA, Edden RA. In vivo magnetic resonance spectroscopy of GABA: a methodological review. Prog Nucl Magn Reson Spectrosc. 2012;60:29–41.
37. Ende G. Proton magnetic resonance spectroscopy: relevance of glutamate and GABA to neuropsychology. Neuropsychol Rev. 2015;25(3):315–25.
38. O'Gorman RL, Michels L, Edden RA, Murdoch JB, Martin E. In vivo detection of GABA and glutamate with MEGA-PRESS: reproducibility and gender effects. J Magn Reson Imaging. 2011;33(5):1262–7.
39. Keefe RS, Harvey PD, Goldberg TE, Gold JM, Walker TM, Kennel C, et al. Norms and standardization of the brief assessment of cognition in schizophrenia (BACS). Schizophr Res. 2008;102(1–3):108–15.
40. Lewis DA, Hashimoto T, Volk DW. Cortical inhibitory neurons and schizophrenia. Nat Rev Neurosci. 2005;6(4):312–24.
41. Hines RM, Hines DJ, Houston CM, Mukherjee J, Haydon PG, Tretter V, et al. Disrupting the clustering of GABAA receptor alpha2 subunits in the frontal cortex leads to reduced gamma-power and cognitive deficits. Proc Natl Acad Sci U S A. 2013;110(41):16628–33.
42. Witt ST, Laird AR, Meyerand ME. Functional neuroimaging correlates of finger-tapping task variations: an ALE meta-analysis. NeuroImage. 2008;42(1):343–56.
43. Ashendorf L, Horwitz JE, Gavett BE. Abbreviating the finger tapping test. Arch Clin Neuropsychol. 2015;30(2):99–104.
44. Barbas H, Pandya DN. Architecture and intrinsic connections of the prefrontal cortex in the rhesus monkey. J Comp Neurol. 1989;286(3):353–75.
45. Barbas H. Two prefrontal limbic systems: their common and unique features. The association cortex: structure and function. Amsterdam: Harwood Academic Publishers; 1997. p. 99–116.
46. Wijtenburg SA, Knight-Scott J. Reconstructing very short TE phase rotation spectral data collected with multichannel phased-array coils at 3 T. Magn Reson Imaging. 2011;29(7):937–42.
47. Soher BJ, Young K, Bernstein A, Aygula Z, Maudsley AA. GAVA: spectral simulation for in vivo MRS applications. J Magn Reson. 2007;185(2):291–9.
48. Provencher SW. Estimation of metabolite concentrations from localized in vivo proton NMR spectra. Magn Reson Med. 1993;30(6):672–9.
49. Wijtenburg SA, Gaston FE, Spieker EA, Korenic SA, Kochunov P, Hong LE, et al. Reproducibility of phase rotation STEAM at 3T: focus on glutathione. Magn Reson Med. 2014;72(3):603–9.
50. Aufhaus E, Weber-Fahr W, Sack M, Tunc-Skarka N, Oberthuer G, Hoerst M, et al. Absence of changes in GABA concentrations with age and gender in the human anterior cingulate cortex: a MEGA-PRESS study with symmetric editing pulse frequencies for macromolecule suppression. Magn Reson Med. 2013;69(2):317–20.
51. Geramita M, van der Veen JW, Barnett AS, Savostyanova AA, Shen J, Weinberger DR, et al. Reproducibility of prefrontal gamma-aminobutyric acid measurements with J-edited spectroscopy. NMR Biomed. 2011;24(9):1089–98.
52. Rowland LM, Summerfelt A, Wijtenburg A, Du XM, Chiappelli JJ, Krishna N, et al. Frontal glutamate and gamma-aminobutyric acid levels and their associations with mismatch negativity and digit sequencing task performance in schizophrenia. JAMA Psychiatry. 2016;73(2):166–74.
53. Rowland LM, Krause BW, Wijtenburg SA, McMahon RP, Chiappelli J, Nugent KL, et al. Medial frontal GABA is lower in older schizophrenia: a MEGA-PRESS with macromolecule suppression study. Mol Psychiatry. 2016;21(2):198–204.
54. Brasil-Neto JP, McShane LM, Fuhr P, Hallett M, Cohen LG. Topographic mapping of the human motor cortex with magnetic stimulation: factors affecting accuracy and reproducibility. Electroencephalogr Clin Neurophysiol. 1992;85(1):9–16.
55. Schutter DJ, van Honk J. The cerebellum in emotion regulation: a repetitive transcranial magnetic stimulation study. Cerebellum (London, England). 2009;8(1):28–34.
56. Schutter DJ, van Honk J. An electrophysiological link between the cerebellum, cognition and emotion: frontal theta EEG activity to single-pulse cerebellar TMS. NeuroImage. 2006;33(4):1227–31.
57. Pinto AD, Chen R. Suppression of the motor cortex by magnetic stimulation of the cerebellum. Exp Brain Res. 2001;140(4):505–10.
58. Jenkinson N, Miall RC. Disruption of saccadic adaptation with repetitive transcranial magnetic stimulation of the posterior cerebellum in humans. Cerebellum (London, England). 2010;9(4):548–55.
59. Hardwick RM, Lesage E, Miall RC. Cerebellar transcranial magnetic stimulation: the role of coil geometry and tissue depth. Brain Stimul. 2014;7(5):643–9.
60. Cattaneo Z, Renzi C, Casali S, Silvanto J, Vecchi T, Papagno C, et al. Cerebellar vermis plays a causal role in visual motion discrimination. Cortex. 2014;58:272–80.
61. Demirtas-Tatlidede A, Freitas C, Cromer JR, Safar L, Ongur D, Stone WS, et al. Safety and proof of principle study of cerebellar vermal theta burst stimulation in refractory schizophrenia. Schizophr Res. 2010;124(1–3):91–100.
62. Avanzino L, Bove M, Trompetto C, Tacchino A, Ogliastro C, Abbruzzese G. 1-Hz repetitive TMS over ipsilateral motor cortex influences the performance of sequential finger movements of different complexity. Eur J Neurosci. 2008;27(5):1285–91.
63. Kammer T, Puls K, Erb M, Grodd W. Transcranial magnetic stimulation in the visual system. II. Characterization of induced phosphenes and scotomas. Exp Brain Res. 2005;160(1):129–40.
64. Salminen-Vaparanta N, Vanni S, Noreika V, Valiulis V, Moro L, Revonsuo A. Subjective characteristics of TMS-induced phosphenes originating in human V1 and V2. Cereb Cortex. 2014;24(10):2751–60.
65. Farzan F, Barr MS, Wong W, Chen R, Fitzgerald PB, Daskalakis ZJ. Suppression of gamma-oscillations in the dorsolateral prefrontal cortex following long interval cortical inhibition: a TMS-EEG study. Neuropsychopharmacology. 2009;34(6):1543–51.

66. Cannon TD, Hennah W, van Erp TGM, Thompson PM, Lonnqvist J, Huttunen M, et al. Association of DISC1/TRAX haplotypes with schizophrenia, reduced prefrontal gray matter, and impaired short-and long-term memory. Arch Gen Psychiatry. 2005;62(11): 1205–13.
67. Du X, Summerfelt A, Chiappelli J, Holcomb HH, Hong LE. Individualized brain inhibition and excitation profile in response to paired-pulse TMS. J Mot Behav. 2014;46(1):39–48.
68. Sommer M, Classen J, Cohen LG, Hallett M. Time course of determination of movement direction in the reaction time task in humans. J Neurophysiol. 2001;86(3):1195–201.
69. Du X, Kochunov P, Summerfelt A, Chiappelli J, Choa FS, Hong LE. The role of white matter microstructure in inhibitory deficits in patients with schizophrenia. Brain Stimul. 2017;10(2):283–90.
70. Ilmoniemi RJ, Kicic D. Methodology for combined TMS and EEG. Brain Topogr. 2010;22(4):233–48.
71. Semlitsch HV, Anderer P, Schuster P, Presslich O. A solution for reliable and valid reduction of ocular artifacts, applied to the P300 ERP. Psychophysiology. 1986;23(6):695–703.
72. Lachaux J-P, Rodriguez E, Martinerie J, Varela FJ. Measuring phase synchrony in brain signals. Hum Brain Mapp. 1999;8(4): 194–208.
73. Groppe DM, Urbach TP, Kutas M. Mass univariate analysis of event-related brain potentials/fields I: a critical tutorial review. Psychophysiology. 2011;48(12):1711–25.
74. Bullmore ET, Suckling J, Overmeyer S, Rabe-Hesketh S, Taylor E, Brammer MJ. Global, voxel, and cluster tests, by theory and permutation, for a difference between two groups of structural MR images of the brain. IEEE Trans Med Imaging. 1999;18(1):32–42.
75. Groppe DM, Urbach TP, Kutas M. Mass univariate analysis of event-related brain potentials/fields II: simulation studies. Psychophysiology. 2011;48(12):1726–37.
76. Pedroarena C, Llinas R. Dendritic calcium conductances generate high-frequency oscillation in thalamocortical neurons. Proc Natl Acad Sci U S A. 1997;94(2):724–8.
77. Lynch JC, Hoover JE, Strick PL. Input to the primate frontal eye field from the substantia nigra, superior colliculus, and dentate nucleus demonstrated by transneuronal transport. Exp Brain Res. 1994;100(1):181–6.
78. Allen G, McColl R, Barnard H, Ringe WK, Fleckenstein J, Cullum CM. Magnetic resonance imaging of cerebellar–prefrontal and cerebellar–parietal functional connectivity. NeuroImage. 2005;28(1):39–48.
79. Huang YZ, Edwards MJ, Rounis E, Bhatia KP, Rothwell JC. Theta burst stimulation of the human motor cortex. Neuron. 2005;45(2):201–6.
80. Fernandez L, Major BP, Teo WP, Byrne LK, Enticott PG. Assessing cerebellar brain inhibition (CBI) via transcranial magnetic stimulation (TMS): a systematic review. Neurosci Biobehav Rev. 2018;86:176–206.
81. Kujirai T, Caramia MD, Rothwell JC, Day BL, Thompson PD, Ferbert A, et al. Corticocortical inhibition in human motor cortex. J Physiol. 1993;471:501–19.
82. Buzsaki G, Logothetis N, Singer W. Scaling brain size, keeping timing: evolutionary preservation of brain rhythms. Neuron. 2013;80(3):751–64.
83. Pellicciari MC, Veniero D, Miniussi C. Characterizing the cortical oscillatory response to TMS pulse. Front Cell Neurosci. 2017;11:38.
84. Dayan E, Censor N, Buch ER, Sandrini M, Cohen LG. Noninvasive brain stimulation: from physiology to network dynamics and back. Nat Neurosci. 2013;16(7):838–44.
85. Formaggio E, Cavinato M, Storti SF, Tonin P, Piccione F, Manganotti P. Assessment of event-related EEG power after single-pulse TMS in unresponsive wakefulness syndrome and minimally conscious state patients. Brain Topogr. 2016;29(2): 322–33.
86. Pellicciari MC, Ponzo V, Caltagirone C, Koch G. Restored asymmetry of prefrontal cortical oscillatory activity after bilateral theta burst stimulation treatment in a patient with major depressive disorder: a TMS-EEG study. Brain Stimul. 2017;10(1):147–9.
87. Fujisawa S, Amarasingham A, Harrison MT, Buzsaki G. Behavior-dependent short-term assembly dynamics in the medial prefrontal cortex. Nat Neurosci. 2008;11(7):823–33.
88. Traub RD, Whittington MA, Stanford IM, Jefferys JG. A mechanism for generation of long-range synchronous fast oscillations in the cortex. Nature. 1996;383(6601):621–4.
89. Chagnac-Amitai Y, Connors BW. Horizontal spread of synchronized activity in neocortex and its control by GABA-mediated inhibition. J Neurophysiol. 1989;61(4):747–58.
90. Yuste R, MacLean JN, Smith J, Lansner A. The cortex as a central pattern generator. Nat Rev Neurosci. 2005;6(6):477–83.
91. Zucker RS, Regehr WG. Short-term synaptic plasticity. Annu Rev Physiol. 2002;64:355–405.
92. Schutter DJ, van Honk J, d'Alfonso AA, Peper JS, Panksepp J. High frequency repetitive transcranial magnetic over the medial cerebellum induces a shift in the prefrontal electroencephalography gamma spectrum: a pilot study in humans. Neurosci Lett. 2003;336(2):73–6.
93. Stoodley CJ, Valera EM, Schmahmann JD. Functional topography of the cerebellum for motor and cognitive tasks: an fMRI study. NeuroImage. 2012;59(2):1560–70.
94. Marvel CL, Desmond JE. The contributions of cerebro-cerebellar circuitry to executive verbal working memory. Cortex. 2010;46(7):880–95.
95. Tomlinson SP, Davis NJ, Morgan HM, Bracewell RM. Cerebellar contributions to verbal working memory. Cerebellum. 2014;13(3):354–61.
96. Ben-Yehudah G, Guediche S, Fiez JA. Cerebellar contributions to verbal working memory: beyond cognitive theory. Cerebellum. 2007;6(3):193–201.
97. Hayter AL, Langdon DW, Ramnani N. Cerebellar contributions to working memory. NeuroImage. 2007;36(3):943–54.
98. Oliveri M, Torriero S, Koch G, Salerno S, Petrosini L, Caltagirone C. The role of transcranial magnetic stimulation in the study of cerebellar cognitive function. Cerebellum. 2007;6(1):95–101.
99. Tomlinson SP, Davis NJ, Bracewell RM. Brain stimulation studies of non-motor cerebellar function: a systematic review. Neurosci Biobehav Rev. 2013;37(5):766–89.
100. Gountouna VE, Job DE, McIntosh AM, Moorhead TW, Lymer GK, Whalley HC, et al. Functional magnetic resonance imaging (fMRI) reproducibility and variance components across visits and scanning sites with a finger tapping task. NeuroImage. 2010;49(1):552–60.
101. Manto M, Bower JM, Conforto AB, Delgado-Garcia JM, da Guarda SN, Gerwig M, et al. Consensus paper: roles of the cerebellum in motor control—the diversity of ideas on cerebellar involvement in movement. Cerebellum. 2012;11(2):457–87.
102. Ugawa Y, Uesaka Y, Terao Y, Hanajima R, Kanazawa I. Magnetic stimulation over the cerebellum in humans. Ann Neurol. 1995;37(6):703–13.
103. Floyer-Lea A, Wylezinska M, Kincses T, Matthews PM. Rapid modulation of GABA concentration in human sensorimotor cortex during motor learning. J Neurophysiol. 2006;95(3):1639–44.
104. Stagg CJ, Wylezinska M, Matthews PM, Johansen-Berg H, Jezzard P, Rothwell JC, et al. Neurochemical effects of theta burst stimulation as assessed by magnetic resonance spectroscopy. J Neurophysiol. 2009;101(6):2872–7.
105. Dubin MJ, Mao X, Banerjee S, Goodman Z, Lapidus KA, Kang G, et al. Elevated prefrontal cortex GABA in patients with major depressive disorder after TMS treatment measured with proton

magnetic resonance spectroscopy. J Psychiatry Neurosci. 2016;41(3):E37–45.
106. Fellous JM, Sejnowski TJ. Cholinergic induction of oscillations in the hippocampal slice in the slow (0.5-2 Hz), theta (5-12 Hz), and gamma (35-70 Hz) bands. Hippocampus. 2000;10(2):187–97.
107. Basar E, Guntekin B. A review of brain oscillations in cognitive disorders and the role of neurotransmitters. Brain Res. 2008;1235: 172–93.
108. Forkel SJ, Thiebaut de Schotten M, Kawadler JM, Dell'Acqua F, Danek A, Catani M. The anatomy of fronto-occipital connections from early blunt dissections to contemporary tractography. Cortex. 2014;56:73–84.
109. Batini C, Compoint C, Buisseret-Delmas C, Daniel H, Guegan M. Cerebellar nuclei and the nucleocortical projections in the rat: retrograde tracing coupled to GABA and glutamate immunohistochemistry. J Comp Neurol. 1992;315(1):74–84.
110. Kwong WH, Chan WY, Lee KK, Fan M, Yew DT. Neurotransmitters, neuropeptides and calcium binding proteins in developing human cerebellum: a review. Histochem J. 2000;32(9):521–34.
111. Wulff P, Ponomarenko AA, Bartos M, Korotkova TM, Fuchs EC, Bahner F, et al. Hippocampal theta rhythm and its coupling with gamma oscillations require fast inhibition onto parvalbumin-positive interneurons. Proc Natl Acad Sci U S A. 2009;106(9): 3561–6.
112. Gonzalez-Burgos G, Hashimoto T, Lewis DA. Alterations of cortical GABA neurons and network oscillations in schizophrenia. Curr Psychiatry Rep. 2010;12(4):335–44.
113. Muthukumaraswamy SD, Edden RA, Jones DK, Swettenham JB, Singh KD. Resting GABA concentration predicts peak gamma frequency and fMRI amplitude in response to visual stimulation in humans. Proc Natl Acad Sci U S A. 2009;106(20):8356–61.